

Resonances in two-magnon Raman spectra and the effect of several exchange parameters*

P. D. Loly, B. J. Choudhury, and W. R. Fehlner[†]

Department of Physics, University of Manitoba, Winnipeg, Manitoba, Canada R3T 2N2

(Received 5 November 1974)

The first calculations of two-magnon Raman line shapes to fully incorporate second-neighbor exchange and all magnon-magnon interactions are reported. Using a spin-orbit coupling mechanism for the excitation of two spin deviations on a single site of a fcc Heisenberg ferromagnet at $T = 0^\circ\text{K}$, we find a resonance well inside the two-magnon band which is qualitatively similar to that seen in antiferromagnets. This resonance is located close to the Ising energy of two spin deviations on a single site, in contrast to the antiferromagnetic situation where the excitations are usually created on neighboring sites for which the resonance is close to the Ising bound-state energy. The line shape and its position are shown to be sensitive to the ratio, $\eta = J_2/J_1$, of exchange parameters for nearest- and next-nearest-neighbor interactions. This sensitivity is illustrated through plots of spectra for $\eta = 0, \pm 0.25$ for $S = 1$ and $S = 7/2$. The latter spin value affords an opportunity to assess the observational prospects for EuO. The effect of finite temperatures is discussed and a second resonance predicted in view of the existence of a resonance in the one-magnon propagator at finite temperature. For a nearest-neighbor sc ferromagnet this secondary resonance should occur at a higher frequency than the primary resonance that we have found at $T = 0^\circ\text{K}$. The relationship between Raman resonances and two-magnon bound states is discussed in the light of results for ferromagnets and antiferromagnets. It is anticipated that new progress can be made in respect of distant-neighbor interactions in antiferromagnets by using a similar computational approach to calculate the appropriate lattice Green's functions.

I. INTRODUCTION

Studies of two-magnon Raman scattering have concentrated almost exclusively on antiferromagnetic insulators for which much experimental data are available.¹ Early attempts to understand the observations were based on the magnon density of states for which it was found necessary to invoke long-range interactions in order to account for experimental line shapes.² A dramatic shift of emphasis followed the 1968 calculations of Elliott and Thorpe³ for nearest-neighbor (nn) antiferromagnets. They demonstrated that magnon-magnon interactions produced a resonance which caused a major distortion of the density of states and showed that the resultant spectrum gave good agreement with observations on RbMnF_3 .⁴ Subsequent work has concentrated on investigating the temperature dependence of the spectrum taking into account magnon renormalization and lifetime effects⁵ within the nn approximation. Little appears to have been done to investigate the limitations of the nn calculations by incorporating the effects of distant shells of neighbors, probably due in part to computational problems which we have been able to overcome. Since it is known that the basic frequency spectra are very sensitive⁶ to second-neighbor interactions, calculations of two-magnon Raman spectra are re-examined in this paper.

We report two new results from calculations of two-magnon Raman line shapes. The first result is the existence of a resonance similar in many respects to that found in antiferromagnets. The other

result concerns the sensitivity of the line shape and the position of its peak to the ratio of next- (second) nearest-neighbor (nnn) to nn exchange interactions. The system investigated involves the generation by one photon, through a spin-orbit mechanism,⁷ of two units of spin deviation on one spin site in a Heisenberg ferromagnet at $T = 0^\circ\text{K}$. These deviations propagate as two spin waves with wave vectors \vec{k} and $-\vec{k}$ and interact strongly because of their excitation on the same spin site. An exact formulation in terms of spin Green's functions for an arbitrary number of exchange parameters incorporates all magnon-magnon interactions and is complemented by accurate computations.

The type of study carried out in this paper for a ferromagnet has considerable relevance for two-magnon Raman studies of antiferromagnets because of the many similarities existing between the properties of systems with these types of magnetic ordering. In general, calculations for antiferromagnets are more complicated than for ferromagnets. The main difficulties arise because the Néel state of fully aligned spins is not an eigenstate of the Heisenberg Hamiltonian and this creates difficulties for the description of the one-magnon state. It follows that the study of two-magnon states will be even less amenable to analysis. All this contrasts with the situation for Heisenberg ferromagnets where the ground state is known, where the one-magnon state is an eigenstate of the Hamiltonian and where the two-magnon problem is exactly soluble in any number of dimensions. Two-magnon bound states were first found in the nn sc ferromag-

net by Wortis⁸ and more recently in the nn bcc case by Bonnot and Hanus.⁹ These bound states exist in nn sc and bcc isotropic ferromagnets only when the total wave vector (\vec{K}) of the magnon pair is greater than a critical value which is close to the Brillouin-zone boundary, albeit depending on the direction in reciprocal space. To date these bound states have only been located for a single high-symmetry \vec{K} direction in the cases cited. It is worth noting that Boyd and Callaway¹⁰ have shown that the bound state connects to a resonance for \vec{K} below the critical wave vector. The corresponding situation in anti-ferromagnets suffers from a lack of comparable information.¹¹

The two-magnon Raman cross section is formulated in terms of spin Green's functions¹² and reduced to a convenient calculational form in Sec. II. Numerical results for the fcc ferromagnet for a range of second-neighbor interactions are given in Sec. III, with a discussion of the results, their implications, and a discussion of unsolved questions given in Sec. IV.

II. FORMULATION

The Hamiltonian describing the ferromagnet is taken to be of the isotropic Heisenberg form,

$$H = -\frac{1}{2} \sum_{i,\delta} J_\delta \vec{S}_i \cdot \vec{S}_{i+\delta}, \quad (1)$$

where the exchange interactions J_δ act between sites whose separation is described by a vector $\vec{\delta}$. J_1 will be used to indicate the nn exchange parameter and J_2 used for *nmn* interactions. The spin operators in (1) obey the usual commutation relations.

We make use of the Green's-function approach initiated by Wortis¹² and with some modifications follow the spirit of the formulation used by Thorpe⁷ in his earlier attempt at the ferromagnetic two-magnon problem. The modifications include generalization to arbitrary range of interaction (instead of a nn restriction) and the use of a more convenient and dimensionless normalization of all Green's functions. We define zero-temperature Green's functions by

$$G_{\delta,\delta'} = (J_1/4SN) \langle\langle A_\delta^\dagger; A_{\delta'} \rangle\rangle, \quad (2)$$

with

$$A_\delta = \sum_i S_i^+ S_{i+\delta}^-. \quad (3)$$

The Raman cross section due to the excitation of two-spin deviations on a single site by a spin-orbit coupling mechanism has been shown by Thorpe⁷ to be proportional to the imaginary part of $G_{0,0}(\omega)$. Though it turns out that $G_{0,0}(\omega)$ can be obtained by restricting consideration to the set of $G_{\delta,0}$'s, we will write down the equation of motion for the more general $G_{\delta,\delta'}$ before making the restriction.

The equation of motion is written as

$$\omega G_{\delta,\delta'} = \langle 0 | [A_\delta^\dagger; A_{\delta'}] | 0 \rangle + \langle\langle [A_\delta^\dagger, H]; A_{\delta'} \rangle\rangle, \quad (4)$$

for which the inhomogeneous part is straightforwardly evaluated. However, at first sight, the homogeneous part appears to introduce Green's functions of the form $\langle\langle S_i^z A_\delta^\dagger; A_{\delta'} \rangle\rangle$ due to $[A_\delta^\dagger, H]$ yielding S_i^z operators. Fortunately at zero temperature these new Green's functions reduce identically to $S G_{\delta,\delta'}$, as can be seen by using $\langle 0 | S_i^z | 0 \rangle = \langle 0 | S$ in the spectral representation

$$\langle\langle A; B \rangle\rangle = \sum_i \left(\frac{\langle 0 | A | i \rangle \langle i | B | 0 \rangle}{\omega - E_i + E_0} - \frac{\langle 0 | B | i \rangle \langle i | A | 0 \rangle}{\omega + E_i - E_0} \right). \quad (5)$$

The final form of the equation of motion consists of a closed set of equation for $G_{\delta,\delta'}$,

$$\begin{aligned} \omega G_{\delta,\delta'} &= (J_1/4SN) N(2S)^2 (\delta_{\delta,\delta'} + \delta_{\delta,-\delta'}) (1 - \delta_{\delta',0}/2S) \\ &+ 2S \sum_x J_x G_{\delta,\delta'} - 2S \sum_x J_{\vec{x}-\vec{\delta}} G_{x,\delta'} - J_\delta G_{\delta,\delta'} \\ &+ \sum_x J_x G_{x,\delta'} \delta_{\delta,0}. \end{aligned} \quad (6)$$

The fourth and fifth terms on the right-hand side of (7) represent spin-wave interactions, as does the $\delta_{\delta',0}/2S$ contribution to the first term (incorrectly printed without the prime in Thorpe's paper¹³). For the set of $G_{\delta,0}$'s the first term on the right-hand side of (6) simplifies to $2SJ_1\delta_{\delta,0}(1 - 1/2S)$.

Dropping all interaction effects enables the resulting equation for the unperturbed Green's functions (denoted by superscript 0) to be solved by Fourier transformation, with the result that $G_{\delta,0}^0$ may be written as a dimensionless lattice Green's function (LGF) g_δ ,

$$G_{\delta,0}^0 = g_\delta = \left(\frac{2SJ_1}{N} \right) \sum_k \frac{e^{i\vec{k}\cdot\vec{\delta}}}{\omega - 2\omega_k}. \quad (7)$$

Translational symmetry tells us that

$$G_{\delta,\delta'}^0 = G_{\delta-\delta',0}^0 = g_{\delta-\delta'},$$

and in (7) the single-magnon dispersion function ω_k is given by

$$\omega_k = S [J(0) - J(k)], \quad (8)$$

with

$$J(k) = \sum_\delta J_\delta e^{i\vec{k}\cdot\vec{\delta}}. \quad (9)$$

Although the equation of motion of $G_{\delta,0}$ is seen from (6) to include only Green's functions of the same order, the third term in (6) generates $G_{x+\delta,0}$'s in contrast to the fifth term which generates only $G_{x,0}$'s (x specifies the set of exchange interactions which are operative). For that reason the equation

of motion does not terminate on its own accord for a finite range of exchange interactions. Fortunately a set of Dyson equations can be constructed from the equation of motion of the $G_{\delta,0}$ and these constitute a finite set of equations for the specification of $G_{\delta,0}$, which is the goal of this section.

The Dyson equations are constructed by recognizing that the equation of motion contains the self-energy part of the Dyson equation. This can be seen by representing the equation of motion as a generalized form of the basic mathematical problem. If D represents a differential operator and we explicitly separate the interaction terms from the noninteracting ones, then

$$DG(x, x') = (1 - 1/2S)\delta(x - x') + [V_0(x) + V_I(x)]G(x, x'),$$

where we explicitly include a factor of $(1 - 1/2S)$ in respect of interaction contributions to the first term of (6). The unperturbed Green's function satisfies

$$[D - V_0(x)]G^0(x, x') = \delta(x - x'),$$

and the solution of the perturbed problem is then given by

$$G(x, x') = (1 - 1/2S)G^0(x, x') + \int dx'' G^0(x, x'')V_I(x'')G(x'', x').$$

Carrying out the same approach in the notation of (6) we have immediately that

$$G_{\delta,0} = (1 - 1/2S)G_{\delta,0}^0 + \left(\frac{1}{2SJ_1}\right) \sum_{\delta''} G_{\delta,0}^0 \times \left(-J_{\delta''}G_{\delta'',0} + \sum_x J_x G_{x,0} \delta_{\delta'',0}\right), \quad (10)$$

which may be rewritten

$$G_{\delta,0} = (1 - 1/2S)g_{\delta} + \left(\frac{1}{2SJ_1}\right) \sum_{\delta'} J_{\delta'}(g_{\delta} - g_{\delta-\delta'})G_{\delta',0}. \quad (11)$$

For the nn case $G_{0,0}$ is completely specified by the Dyson equations for $G_{0,0}$ and $G_{1,0}$ while the nnn case requires the addition of $G_{2,0}$. It is also possible to drop one of the Dyson equations and use the equation of motion of $G_{0,0}$ in its place, but we prefer to use the full set of Dyson equations which give a more direct picture of the effect of interactions on the unperturbed spectrum (as we will see later).

In the nn fcc case the Dyson equations involve five LGF's g_0 to g_4 , labeled by δ 's given in units of $\frac{1}{2}a$ by $(0, 0, 0)$, $(1, 1, 0)$, $(2, 0, 0)$, $(2, 1, 1)$, and $(2, 2, 0)$, respectively. In the nnn case g_5 and g_6 also arise, corresponding to $(3, 1, 0)$ and $(4, 0, 0)$, respectively. Fortunately a set of identities relating many of the LGF's can be constructed for all lattices and arbitrary range of interaction by

first rewriting the orthogonality property

$$\frac{1}{N} \sum_k e^{i\mathbf{k}\cdot\delta_i} = \delta_{i,0} \quad (12)$$

in the following manner:

$$\delta_{i,0} = \frac{1}{N} \sum_k \frac{e^{i\mathbf{k}\cdot\delta_i}(\omega - 2\omega_k)}{\omega - 2\omega_k}. \quad (13)$$

Then expanding the ω_k in the numerator with the help of (8) and (9), we find that

$$\delta_{i,0} = \left(\frac{\omega}{2SJ_1} - \sum_i \eta_i Z_i\right)g_i + \sum_j \eta_j Z_j h_{i,j}, \quad (14)$$

where $\eta_i = J_i/J_1$ and $h_{i,j} = h_{j,i}$ being defined by

$$h_{i,j} = (Z_j)^{-1} \sum_{\delta_j} g_{\delta_j} \delta_{i-\delta_j}, \quad (15)$$

where the sum in (15) is over the set of vectors reached by the i th J_0 . With this notation the usefulness of the identities is readily seen if the second term on the right-hand side of the Dyson equations of (11) is rewritten using $\sum_i \sum_{\delta_i}$ instead of $\sum_{\delta'}$, giving

$$\left(\frac{1}{2SJ_1}\right) \sum_i J_i \left(g_{\delta} Z_i - \sum_{\delta_i} g_{\delta-\delta_i}\right)G_{i,0}, \quad (16)$$

so that (15) then gives the Dyson equation an explicit dependence on a group of LGF's through h_{δ,δ_i} , i. e.

$$\left(\frac{1}{2SJ_1}\right) \sum_i Z_i J_i (g_{\delta} - h_{\delta,\delta_i})G_{i,0}. \quad (17)$$

For the fcc lattice the identities relating various LGF's enable a reduction to one LGF in the nn case (either g_0 or g_1) and a minimum of four LGF's in the nnn case.

Before embarking on numerical calculations for specific cases it is useful to consider constraints on the final spectrum which are useful in interpreting the results. We can derive sum rules for the integrated Raman intensity, proportional to $\text{Im}G_{0,0}(\omega)$, and its moments in the following manner. Firstly g_0 and g_6 are expanded *within* the two-magnon band in inverse powers of frequency yielding

$$g_0 = 2SJ_1 \left(\frac{1}{\omega} + \frac{2S \sum_i J_i Z_i}{\omega^2} + O(\omega^{-3})\right) \quad (18)$$

and

$$g_6 = 2SJ_1 [-2SJ_6/\omega^2 + O(\omega^{-3})]. \quad (19)$$

Using these in the Dyson equations it follows directly that

$$G_{\delta,0}(\omega) \sim \omega^{-2} \text{ for } \delta \neq 0. \quad (20)$$

Then from the Dyson equation for $G_{0,0}$ we have

$$G_{0,0} = (1 - 1/2S)2SJ_1 \left(\frac{1}{\omega} + \frac{2S \sum_i J_i Z_i}{\omega^2} + O(\omega^{-3})\right). \quad (21)$$

Taking the imaginary part of $G_{0,0}(\omega)$ and making use of the identity

$$1/(\omega + i\epsilon) = P(1/\omega) - i\pi\delta(\omega) \quad (22)$$

together with the integral properties of the δ function leads finally to an integrated intensity sum rule,

$$(-) \int_{-\infty}^{\infty} \text{Im}[G_{0,0}(\omega)] d\omega = (2SJ_1)\pi(1 - 1/2S), \quad (23)$$

and a first-moment sum rule,

$$(-) \int_{-\infty}^{\infty} \text{Im}[G_{0,0}(\omega)] \omega d\omega = (2SJ_1)\pi(1 - 1/2S) \times 2S \left(\sum_i J_i Z_i \right). \quad (24)$$

Higher moments can be derived if the need should arise.

Another property of the final spectrum results from recognizing that the Dyson equation of (11) and the spin dependence (for corresponding frequencies, ω/S constant) of the g_6 's and $G_{6,0}$'s allow us to write $G_{0,0}(\omega)$ in the form of an unperturbed spectrum plus an effect due to spin-wave interactions,

$$G_{0,0}(\omega) = (1 - 1/2S)[g_0(\omega) + (1/S)R(\omega)]. \quad (25)$$

In general $R(\omega)$ is a complicated function which for large S is a slowly varying function of $1/S$. We illustrate this for the nn case for which (11) and (25) give

$$R(\omega) = Z_1 g_1 (g_0 - g_1) / 2 \left(1 - \frac{\omega}{2SJ_1} \frac{g_1}{2S} \right) \quad (26)$$

$$= \frac{1}{2} Z_1 g_1 (g_0 - g_1) \left[1 + \left(\frac{\omega}{2SJ_1} \right) \frac{g_1}{2S} + O(S^{-2}) \right], \quad (27)$$

with the g_6 's being independent of spin for constant ω/S . Equation (25) shows that the interaction effects are greatest for small spin and absent for $S = \infty$.

III. RESULTS

Specific calculations are reported in this section for the nnn fcc case for a range of values of $\eta = J_2/J_1$ which represent the range suggested for EuO. We also give the nn spectrum which acts as a reference for the effect of nnn interactions and also corrects Thorpe's earlier calculation.

The main difficulty in the numerical calculation is associated with the LGF's. Although the real and imaginary parts of the basic lattice Green's functions g_6 are readily available for the nn ferromagnetic case, the required information is not available in the nnn case.¹⁴ The imaginary part involves a surface integral in much the same way as the density-of-states problem, while the real part contains a volume integral of an integrand which contains

singular surfaces. Though it is possible to obtain the real part by a Hilbert transform of the imaginary part, the latter would have to be extremely accurate for that procedure to be successful. In another investigation¹⁵ two of us (W. R. F. and P. D. L.) have developed a powerful method (SAVE) for the direct numerical integration of the Brillouin-zone sums for the real and imaginary parts of LGF's. SAVE can be used with any desired dispersion function so that it is not restricted by the number of exchange parameters or the type of magnetic ordering. The results presented in this paper used an overall accuracy of about 1% for the LGF data. This gives good resolution of the Van Hove singularities and was considered quite adequate for the investigations undertaken, though if desired the residual errors could be reduced substantially by increasing the computer time used.

A measure of the adequacy of the LGF data is offered by testing the sum rules for the final spectrum, shown in Fig. 1. These were given in (23) and (24) and are found to be satisfied in all cases to within the same accuracy as the LGF data used in calculating the spectra. This is in contrast to Thorpe's results for the nn fcc case which gave a large deficit (about 30% for $S=1$) in the first sum rule, which he attributed to the existence of a two-magnon bound state above the continuum. Indeed, Thorpe was able to pin down the weight and position of that bound state by using the sum rules. Though we now know of the errors in his formulation it is perhaps interesting to note that in the nn sc case Thorpe⁷ found the sum rules to be satisfied, consistent with the known absence of bound states at $\vec{K} = 0$ in that case. Having repeated the nn sc calculations ourselves, finding a spectrum qualitatively similar to the fcc results given in Fig. 1, and also having regenerated Thorpe's result, we can confirm that the incorrect spectrum satisfies the sum rules almost as well as the correct result. Of course one would expect a distinction to occur for higher moments.

It is clear that for finite spin the correction effect to the unperturbed spectrum defined in (25) redistributes the weight in the spectrum in a manner such that the sum rules are conserved, while the total area under $\text{Im}G_{0,0}(\omega)$ varies with S as $(1 - 1/2S)$ in accord with (23). The imaginary part of $R(\omega)$, which can be obtained by subtracting the $(1 - 1/2S)$ weighted $S = \infty$ curves in Fig. 1 from those for finite spin, exhibits a well defined resonance effect within the two-magnon band which reduces weight at the top and bottom of that band. Considering the spin dependence for $\eta = -0.25$ from Fig. 1 we see that the resonance dominates the spectra for $S=1$, is absent for $S = \infty$, but with the peak for $S = \frac{1}{2}$ being determined by a competition between the resonance, $\text{Im}R(\omega)$, and the two-magnon density of states

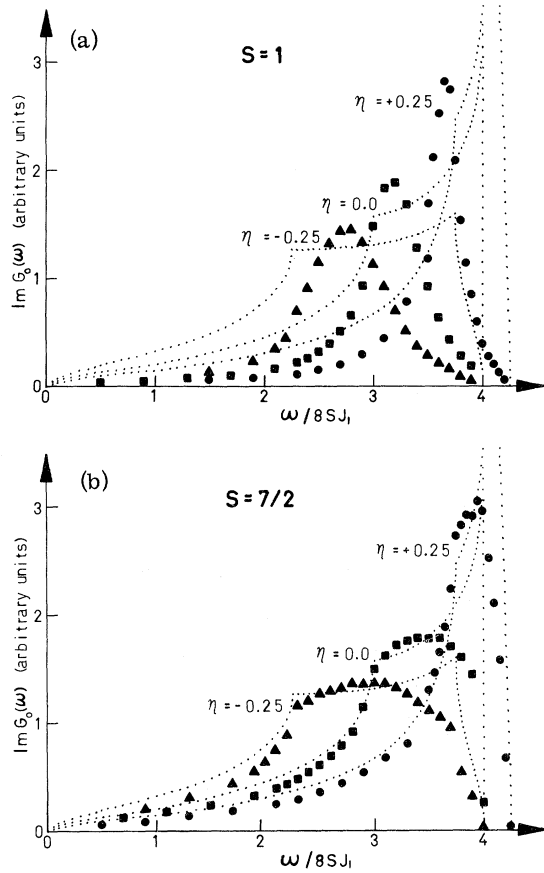


FIG. 1. Calculated two-magnon Raman spectra for three values of η , the ratio of J_2/J_1 , as a function of frequency. Points in Fig. 1 (a) for $S=1$ and Fig. 1 (b) for $S=7/2$ are shown for $\eta=-0.25$ (solid triangles), $\eta=0.0$ (solid squares), and $\eta=+0.25$ (solid circles). In both Fig. 1 (a) and Fig. 1 (b) the basic two-magnon density of states scaled by $(1-1/2S)$, are shown as dotted lines for the three η values; for $\eta=0.0$ a logarithmic singularity occurs at $\omega/8SJ_1=4.0$, while for $\eta=+0.25$ the upper end is not shown but peaks sharply at a value of 4.25 at $\omega/8SJ_1=4.166$ (see Ref. 6).

$\text{Im}G_0(\omega)$. Also as the spin is reduced and the magnon-magnon interactions strengthen the resonance, the Van Hove singularities become less conspicuous features of the spectra. It is furthermore implicit in the results in Fig. 1 that the position of the resonance is essentially independent of spin for constant ω/S .

The position of the resonance peak is very close to the energy of two spin deviations on a single site as calculated from the Ising portion of the Heisenberg Hamiltonian in (1), being given by $2S(Z_1J_1 + J_2J_2)$. We note that this energy is also the energy of two spin deviations which are separated by a greater range than the exchange interactions. In the nn antiferromagnetic case, for the creation of

spin deviations on nearest-neighbor sites by an exchange coupling mechanism, a qualitatively similar resonance was found by Elliott and Thorpe³ near the energy of the corresponding Ising bound state which is lower than the separated Ising energy by J_1 .

IV. DISCUSSION

We have demonstrated the feasibility of going beyond the nn approximation in calculating two-magnon Raman spectra. Through calculations for a nnn fcc ferromagnet we have shown that the sensitivity of the line shape to details of the nnn interactions is large enough that any analysis of measured spectra which neglects them when they are appreciable would be misleading. It also follows from our ability to calculate distant-neighbor LGF's that it is now feasible to make new progress on the corresponding antiferromagnetic problem. Such an extension of existing nn calculations may contribute to removing the remaining discrepancies for RbMnF_3 and other materials at low temperatures. We also expect that similar possibilities will occur for exciton-magnon sidebands.¹⁶

The sensitivity of the peak position and width to variations in η is dramatically shown in Fig. 1(a) for $S=1$ and follows roughly the variation of $\text{Im}G_0(\omega)$, the $S=\infty$ limit. The curves for $S=7/2$ in Fig. 1(b) represent the range of η values estimated by a number of workers for EuO. Although the sign and magnitude of J_2 for EuO is in question,¹⁷ it is clear that calculations of two-magnon Raman spectra without its inclusion would have very little value. It must be remembered that only one mechanism has been discussed here for ferromagnets and if another existed, which created spin deviations on neighboring sites, the interpretation of spectra would be more complicated. In cases where the present spin-orbit mechanism dominates there is a good prospect of settling the question of J_2 . A recent attempt¹⁸ to observe this spectrum for EuO failed because of a lack of stoichiometry which gave a large first-order effect. Hopefully, improved specimens will exhibit the second-order spectrum. In respect of other ferromagnetic candidates for the observation of two-magnon Raman spectra, Tb has been proposed¹⁹ because its density of states, having a well defined peak near the upper band edge rather akin to the present $\eta=0.25$ case, would enhance its prospects of being resolved.

At finite temperatures three principal effects are introduced. Firstly, bare magnon energies will decrease with increasing temperature according to the self-consistent renormalization theory²⁰ up to near T_c , causing an appropriate scaling of the spectrum to a smaller bandwidth. Secondly, lifetime effects will soften sharp features in the spectrum. Finally, noting that Silberglitt and Harris²¹ have established a resonance in the one-magnon

propagator of the nn sc ferromagnet at nonzero temperature, a second resonance would presumably be present in the two-magnon spectrum at finite temperatures. This second resonance occurs at 78° along the (1, 1, 1) direction of the sc Brillouin zone, or about $\frac{3}{4}$ of the maximum one-magnon energy, and we therefore expect it to be located above the primary resonance discussed in this paper.

Finally, it seems appropriate to make some remarks about resonances in two-magnon Raman spectra and their relationship to any bound states of two-magnons which may exist in the same systems. Apart from the bound states mentioned in Sec. I, the only other examples occur in the presence of anisotropy. Nevertheless, since a correlation has been noted¹³ between the antiferromagnetic resonance and the Ising bound-state energy, the question of their relationship naturally arises. Owing to a shortage of information hitherto, no further light has been shed on this problem. However, by drawing on the additional information obtained in the present paper, together with preliminary results that two of²² us (B. J. C. and P. D. L.) have obtained for anisotropic extensions of this

work, we feel that a tentative discussion is in order at this time. Two-magnon Raman spectra, whether for single-site or neighboring-site generation of two spin deviations, may be regarded as a probe of two-magnon excitations for zero total momentum of the pair ($\vec{K}=0$). The answer to the relationship between bound states and resonances will eventually require that the gap between $\vec{K}=0$ and the large \vec{K} region where the bound states exist be bridged. Until a suitable probe is found it appears to be profitable to explore anisotropic effects which yield a bound state at $\vec{K}=0$. It is then possible to see how the resonance makes a transition to the bound state by varying the anisotropy. One related point that should be recognized is that the fcc case is not going to be as straightforward to understand as either the sc or bcc cases. This follows because a simple analysis of the extent of the two-magnon continuum for the nn fcc ferromagnet, whose spectra are shown in Fig. 1, gives a minimum width which encompasses the Ising bound-state energy in a similar fashion to the nn antiferromagnet and therefore seems to preclude sharply defined bound states for that case.

*Research supported by the National Research Council of Canada.

†Present address: Department of Physics, Erindale College and University of Toronto, Mississauga, Ontario.

¹See the review by P. A. Fleury and S. P. S. Porto [J. Appl. Phys. **39**, 1035 (1968)].

²S. J. Allen, Jr., R. Loudon, and P. L. Richards, Phys. Rev. Lett. **16**, 463 (1966).

³R. J. Elliott, M. F. Thorpe, G. F. Imbusch, R. Loudon, and J. B. Parkinson, Phys. Rev. Lett. **21**, 147 (1968); R. J. Elliott and M. F. Thorpe, J. Phys. C **2**, 1630 (1969).

⁴P. A. Fleury, Phys. Rev. Lett. **21**, 151 (1968).

⁵R. W. Davies, S. R. Chinn, and H. J. Zeiger, Phys. Rev. B **4**, 992 (1971).

⁶P. D. Loly and M. Buchheit, Phys. Rev. B **5**, 1986 (1972); P. D. Loly, Phys. Rev. B **8**, 4405 (1973).

⁷M. F. Thorpe, Phys. Rev. B **4**, 1608 (1971). Part of this formulation and all the results are in error.

⁸M. Wortis, Phys. Rev. **132**, 85 (1963); see also J. Hanus, Phys. Rev. Lett. **11**, 336 (1963).

⁹A. M. Bonnot and J. Hanus, Phys. Rev. B **7**, 2207 (1973); see also A. W. Saenz and W. W. Zachary, J. Math. Phys. **14**, 1837 (1973).

¹⁰R. G. Boyd and J. Callaway, Phys. Rev. **138**, A1621 (1965).

¹¹R. J. Elliott and A. J. Smith, J. Phys. (Paris) **32**, C1-585 (1971).

¹²M. Wortis, Phys. Rev. **138**, A1126 (1965).

¹³One error in Ref. 7 has been noted in Ref. 9. All errors are corrected in our work and the final spectrum

satisfies the sum rules for all cases considered in this article, in contrast to the nn result in Ref. 7.

¹⁴Some of the needed LGF's have been calculated and tabulated in a compact Chebyshev representation by R. H. Swendsen and H. Callen [Phys. Rev. B **6**, 2860 (1972)]. Unfortunately the tables do not reproduce the basic data faithfully, introducing severe discontinuities, probably due to a lack of significant figures in the Chebyshev coefficients.

¹⁵W. R. Fehlner and P. D. Loly, Solid State Commun. **15**, 69 (1974). SAVE is a quasianalytic numerical-integration method differing from that of G. Gilat and L. J. Raubenheimer, [Phys. Rev. **144**, 390 (1966)] in using quadratic expansions over spherical cells instead of linearization over space-filling polyhedra. Advantages over Gilat-Raubenheimer schemes result from simpler logic and a better representation of Van Hove singularities, with no significant disadvantages.

¹⁶See Ref. 3 and J. B. Parkinson and R. Loudon, J. Phys. C **1**, 1568 (1968).

¹⁷L. Passell, O. W. Dietrich, and J. Als-Nielsen, A.I.P. Conf. Proc. **10**, 1251 (1972).

¹⁸A. Schlegel and P. Wachter, Solid State Commun. **13**, 1865 (1973).

¹⁹M. Inoue and T. Moriya, J. Phys. Soc. Jpn. **29**, 117 (1970).

²⁰P. D. Loly, J. Phys. C **4**, 1365 (1971).

²¹R. Silbergliitt and A. B. Harris, Phys. Rev. Lett. **19**, 30 (1967).

²²B. J. Choudhury and P. D. Loly, AIP Conf. Proc. (to be published).